JOURNAL OF AIRCRAFT
Vol. 31, No. 2, March–April 1994

Investigation of Monte Carlo Simulation in FAA Program KRASH

Howard J. Fleisher*
Galaxy Scientific Corporation, Pleasantville, New Jersey 08232
and
Haym Benaroya†
Rutgers University, Piscataway, New Jersey 08855

In 1971, the U.S. Army first supported the development of computer code KRASH to model the impact dynamics and mechanics of airframes. The Federal Aviation Administration continued this support in 1975. Many enhancements have been added to the initial code, and the current official release version is KRASH 85. The next step in the ongoing advancement of KRASH includes uncertainties in modeling capabilities, which is the contribution of this work. In particular, a Monte Carlo simulation framework has been utilized here to permit the input of parameter uncertainties, and thus allow the output variables to be bound with a degree of statistical confidence. An airframe model was selected and preliminary sensitivity tests were performed on four parameters, specifically the impact surface coefficient of dynamic friction, the internal beam damping constant, the external crushing spring damping ratio, and the material properties, including yield stresses. Results from these preliminary tests showed the model was sensitive to variation in the first three parameters, while it was insensitive to changes in the material properties. Accelerations and impulses were plotted for two of the masses in the model. The means and standard deviations at each time step were calculated and incorporated into the plots. Finally, verification whether the simulation yielded statistically significant results, and confidence bounds for results with large uncertainty are presented. The techniques outlined here are completely extendable to as general a KRASH model as desired.

I. Introduction

OVER the past approximately 20 yr, serious concern over product reliability has led to a re-evaluation of traditional engineering design approaches based upon deterministic assumptions. As a result of this concern and consequent research activity, considerable progress has been made in applying probability theory to the general area of engineering mechanics and structural engineering.[1,2]

The objective of this work is to present a means of transforming an existing deterministic code into its probabilistic counterpart. Specifically, the code to be modified and enhanced is the Federal Aviation Administration (FAA) sponsored program KRASH, which is currently the most commonly used computer program in aircraft crash analysis. Two possible methods of performing this transformation are perturbation techniques and Monte Carlo simulation.

Perturbation techniques would require extensive use of the algebra of expectation.[3] This in turn would necessitate extensive rewriting of the current KRASH code, which is undesirable. Conversely, the Monte Carlo simulation method is a probabilistic envelope which can be placed around the existing code. Only modifications to input and output formats would be necessary. For this reason, a Monte Carlo simulation will be used to transform KRASH into a probabilistic tool.

A. Motivation

KRASH is a computer program used to analyze the dynamic response of airframes to a crash impact. The vehicle structure is modeled as a collection of nonlinear beam elements interconnecting lumped masses. The program has recently been used to model transport category aircraft.[4,5] However, running the existing code often requires extensive testing to generate input material property and stiffness data, properties which certainly differ from specimen to specimen.

Since it is apparent that practically all engineering variables exhibit scatter characteristics (meaning they may have a number of different possible values), then in order to more accurately predict the performance of a design, the mathematical models of such functions must also show multivalued random characteristics. Because of this random nature, the value of a particular variable is said to be uncertain. By adding a Monte Carlo simulation to program KRASH, the sensitivity of the system performance to variation in the system parameters may be examined or assessed. This information in turn will permit the identification of parameters/models that need to be better defined so that results can be made more accurate. Furthermore, it is likely that this Monte Carlo capability will reduce the amount of testing currently essential to run KRASH. Additionally, with the bounding of inputs and outputs, test designers will be able to optimize structural experiments to gain as much useful information as possible. Given the time and cost associated with even one test, such a capability is desirable.

B. Contribution of the Work

As the popularity of air travel continues to grow along with the average age of the commercial airline fleet, so too does the incidence of airplane crashes. It therefore becomes imperative to model airframes for crash impact scenarios, particularly for those cases which are severe, but survivable. However, to fully evaluate the appropriateness of crash scenarios for design considerations, it is necessary to predict airframe structure dynamic responses with a reasonable degree of accuracy. This means creating a mathematical (probabilistic) model for input parameter uncertainties, thereby providing improved methods for evaluating and predicting

Received Feb. 18, 1992; revision received Jan. 23, 1993; accepted for publication Feb. 23, 1993.

*Research Engineer, Aviation Division, 2500 English Creek Avenue. Member AIAA.

†Associate Professor of Mechanical and Aerospace Engineering, P.O. Box 909. Associate Fellow AIAA.

airworthiness and crash dynamics, with the ultimate goal being increased passenger survivability.

The Monte Carlo simulation method is a well documented[6-8] and frequently employed technique to probabilistically model parameter uncertainties. The major objective of this work is to utilize this existing methodology to better represent input parameters in program KRASH. This new modeling approach could then be incorporated into the existing code as an optional tool. KRASH will then be capable of estimating bounds on possible structural behavior. This is the first known effort to develop KRASH into a probabilistic tool. In order to make the new probabilistic code even more useful, it is anticipated that it can be ported to the personal computer (PC) environment for individual analysis.

II. KRASH Background

This section summarizes the capabilities of the current official KRASH program (KRASH 85). For a more detailed explanation, the reader is encouraged to see Ref. 8.

A. Introduction

KRASH predicts the response of vehicles to multidirectional crash environments. The program computes the time histories of N interconnected masses, each allowed six degrees of freedom (DOF). The Euler equations of motion are integrated numerically to obtain velocities, displacements, and rotations. Gravitational forces, internal forces and moments, and external forces are computed. For small deflections, a linear analysis is obtained, and for large deflections, general plastic deformation is analyzed. The program provides for unloading and subsequent reloading along a linear-elastic line.

The code describes the interaction between a series of massless interconnecting structural elements and concentrated rigid body masses to which the structural elements are attached at their ends, with the appropriate end fixity. The structural elements can be connected between node points which are offset from and rigidly attached to selected mass points. The interconnecting elements are nonlinear beams which represent the stiffness characteristics of the structure between the masses. The masses can translate and rotate in all directions under the influence of the external forces, as well as the constraining internal beam element forces. Some of the more important capabilities of KRASH are 1) defines the response of six DOF at each representative location; 2) determines mass accelerations, velocities, and displacements; 3) includes internal structural damping; 4) determines when element rupture takes place and redistributes the loading over remaining structural elements; 5) determines the distribution of kinetic and potential energies by lumped mass, the distribution of strain and damping energies by element, and the sliding friction energies associated with each external spring; 6) determines the vehicle response to an initial condition that includes linear and angular velocity about three axes and any arbitrary vehicle attitude; 7) provides a measure of the airplane center-of-gravity (c.g.) velocity; and 8) analyzes a model of up to 80 masses and 150 beam elements.

The following operations can also be performed by KRASH. These capabilities are optional user-defined functions: 1) provides for general nonlinear stiffness properties in the plastic regime and determines the amount of permanent deformation; 2) provides for ground contact by external structure modeled as nonlinear springs; 3) defines mass penetration into an occupiable volume; 4) includes measures of injury potential to the occupants; and 5) computes hydrodynamic forces associated with a water impact (algorithm not in the official KRASH 85 version).

B. Limitations

The first group of limitations in program KRASH affect the size of the model. A maximum size of 80 masses and 150 internal beam elements is allowed, and up to 40 external springs may be used. Additionally, only 10 nonstandard materials may be specified in addition to the 10 materials built into the code. This can cause difficulty if a large number of different materials, especially composites, which are all nonstandard, are used in the model. Another limitation is that structural testing is usually required to generate input data, such as force-deflection properties to model the external springs. This also leads to uncertainties in the input parameters, since these values are highly dependent upon the histories of the sections being evaluated.

An important theoretical limitation with KRASH is the potential for negative strain energies to develop in nonlinear beam elements, which is not possible in a real physical system. This is due to the stiffness reduction factor approach that is the foundation of the user specified load-deflection behavior. Only the coupled nonlinear DOF pose potential problems, however, as linear motion analyses never yields negative strain energy, and the uncoupled DOF are well-behaved even with nonlinearities. Finally, since the strain energy of each beam is part of the output, the user will be aware if negative strain energies develop in any beams in the model. Use of a plastic hinge to analyze nonlinear coupled bending is an alternative offered by the program.

Finally, the models themselves have limitations with regard to matching the level of detail in areas of damage when compared to actual drop test results. For example, the stick model in the CID test could not represent local failures, such as shearing of the webs. The expanded CID model is better able to represent discrete failures, although limitations still exist. Additionally, since one beam represents connectivity between major regions of structure, it is difficult for the models to represent the overall nonlinearities.

III. Monte Carlo Simulation

A. Introduction

The term Monte Carlo was first introduced by von Neumann and Ulam[7] during World War II. Monte Carlo methods were initially used in development of the atomic bomb, where they were applied to problems involving random neutron diffusion in fissile material. Monte Carlo simulation is used to generate estimates of the statistics describing various functions, utilizing statistical descriptions of the involved variables.

The simulation process consists of generating many values of the function of interest by computer calculations. Statistical tests are usually applied to the variable to be modeled to indicate the most likely probability distribution that will produce similar synthesized values. These values are normally obtained directly from already developed programs. Such "random numbers" are called *pseudorandom* because they are attained via deterministic equations. Sets of random values for the simulated variable are required in the Monte Carlo process. Each generated number produces a corresponding result, until a family of results exists for the set of random input variables. Finally, all the results are averaged to obtain a mean value and higher moments, from which confidence bounds can be obtained. It should be mentioned that since Monte Carlo results arise from observational data consisting of random numbers, it is necessary that the family of results be large to ensure convergence to a statistically significant result.

The main drawback to Monte Carlo simulation is that it can often be a computationally time-consuming technique. Despite this problem, and considering the pace at which digital computers are evolving, the Monte Carlo method is now the most powerful and commonly used technique for analyzing complex probabilistic problems. However, the complexity and computational effort required has been increasing, since realism has demanded greater intricacy and more extensive descriptions.[1]

B. Random Number Generation

The most frequently used present-day method for generating pseudorandom numbers is the linear congruential generator. This generator is based on recursive calculations of the residues of modulus m of a linear transformation.[6] Such a recursive relation may be expressed as

$$X_{i+1} = (aX_i + c)(\text{mod } m) \quad (1)$$

where a, c, and m are nonnegative integers.

Such a sequence of pseudorandom numbers is cyclic, and will repeat itself in at most m steps. To ensure randomness, the period of the cycle should be as long as possible, and therefore in practical applications a large value of m should be assigned in the generation of X_i. The selection of values for m, a, and c is the most important step for creating a generator of this sort. Table 1 lists some choices for these constants that will yield a large period. These values have been tested statistically and shown to give satisfactory results.[9]

Here, the random number generation routine decided upon for the Monte Carlo simulation uses three separate linear congruential generators, each employing any one set of constants from Table 1. This is primarily done for two reasons. Two generators are used for the output number, ensuring that the low-order (least significant) bits of the number are as random as the high-order bits. This prevents computer round-off of integer arithmetic, allowing more random behavior. The third generator is used to control a shuffling routine to avoid sequential correlation between numbers. This ensures that the period of the generator is, for all practical purposes, infinite. The choice of which sets of constants to select from Table 1, as well as the size of the randomizing shuffle, is essentially arbitrary. However, the larger the shuffling array, the less likely it is that sequential correlation will occur. Ultimately, this choice must be balanced with computational time and required storage space for the array.

The generator will give a uniformly distributed value on the interval (0, 1). A subroutine was written in FORTRAN, and is taken from Ref. 9. The code follows the procedure outlined above, and the last three sets of constants from Table 1 were selected. The length of the shuffling array was chosen at 100 values. As a test of the subroutine, 10,000 numbers were generated with a standard uniform distribution. No sequential correlation was observed, and the calculated mean and standard deviation were within 0.01% of the expected values.

Table 1 Constants for random number generators

m	a	c
7,875	421	1,663
11,979	859	2,531
21,870	1,291	4,621
81,000	421	17,117
86,436	1,093	18,257
117,128	1,277	24,749
121,500	4,081	25,673
134,456	8,121	28,411
243,000	4,561	51,349
259,200	7,141	54,773

C. Generation of Random Variates

The generation of random variates can be accomplished systematically from the uniform distribution on the interval (0, 1) which was determined in the preceding section. This is done through one of several methods, such as the inverse transform method, composition method, and acceptance-rejection method.[6] Table 2 lists equations to generate random variates for common probability density functions given random values of standard uniform (R_U) and standard normal (R_N) distributions. Standard uniform random values are generated on the interval (0, 1). Since most engineering parameters fall into either the normal, lognormal, or exponential distributions, only these transformations are listed in Table 3.

IV. Model Selection and Sensitivity Analysis

In this section a comparison of models previously used in the Controlled Impact Demonstration (CID) test is made. Based on this comparison, the stick model was selected for use in the Monte Carlo simulation. A sensitivity test was performed on several input parameters to determine which should be incorporated in the simulation. Results of this analysis are presented.

All runs were performed using a VAX execution file because the source code was not available for these studies. The system used was a VAX 8650 processor, which operated under the VAX/VMS operating system. The times listed in Table 3 are run times only. Additional time was needed to modify the input and output files to acceptable formats. Given our results here, however, it appears the source code will become available for future studies.

A. Comparison of Models

Two models were considered for the proposed simulation. The first is the 17 mass, 16 beam CID stick model. Although very basic in structure, the model gives a fundamental understanding of the effects of the simulation on the input parameters. Furthermore, since a large number of runs are necessary for the simulation process, the time required to run the stick model is acceptable. The second model considered is the 48 mass, 137 beam CID expanded model. The benefit of this model is a more detailed analysis. Because of the increased detail of the interconnecting beams, nonlinearities are specified as well. The extra detail obtained from the expanded model, however, carries a much longer run time with it. Both models are shown in Figs. 1 and 2.

The results of the CID test showed generally good agreement between actual test data and the pretest KRASH analysis for both the stick and expanded models. However, the stick model responses were more representative of the floor pulses measured during the CID test than were the expanded model results.[5] This is because the expanded model is not as stiff as the actual airframe, therefore predicting smaller accelerations than are observed from structural test data. Since the primary focus of this study is determining the sensitivity of the floor pulses to parametric variations, use of the stick model provides the most feasible and time-effective approach. Table 4 shows a comparison of run times for each model, further supporting the selection of the CID stick model for this study.

Table 2 Recursive relations to obtain common random variates[10]

Distribution to simulate	Probability density function	Procedure to obtain random value y'
Exponential	$f(y) = \lambda e^{-\lambda(y-\mu)} \mu \le y < \infty$	$y' = -\frac{1}{\lambda} \ln (R_U) + \mu$
Log-normal	$f(y) = \frac{1}{\sqrt{2\pi}\sigma y} \exp\left[-\left(\frac{\ln y - \mu}{2\sigma}\right)^2\right] \quad 0 \le y < \infty$	$y' = e^{\mu + \sigma R_N}$
Normal	$f(y) = \frac{1}{\sigma\sqrt{2\pi}} \exp\left[-\frac{(y-\mu)^2}{2\sigma^2}\right] \quad -\infty < y < \infty$	$y' = \mu + \sigma R_N$

Once the stick model was selected, the next step involved definition of the impact conditions. The choice of conditions was limited by the fact that only the KRASH 85 section of the entire KRASH analysis system was available. The programs not provided were the KRASHIC and MSC/NASTRAN sections.[11] These two codes are normally used if initial beam loads and deflections are nonzero. Because of this restriction, the impact conditions employed had to guarantee that at time zero the beams all had zero internal deflections and loads. This meant that the aerodynamic forces had to be set to zero as well. As a consequence of this, a simple drop test was selected here for the model with the nose slightly up. The sink speed was 17 ft/s, and the nose was slightly elevated at a 1-deg angle. The response was studied for a time of 0.16 s, consistent with the CID test. It should be pointed out, however, that there is no inherent difficulty in implementing the Monte Carlo simulation for any general set of initial conditions consistent with KRASH analysis.

B. Choice of Parameters for Sensitivity Analysis

This section discusses the selection of the parameters to be considered for the Monte Carlo simulation. The sensitivity analysis will show which variables most affect the response of the model. By eliminating those parameters which have little effect on the response, the overall computational time for the Monte Carlo simulation can be minimized.

A large number of the input parameters used in program KRASH exhibit scattered behavior. Those upon which this study focuses represent fuselage and interior structural characteristics. In particular, the list of variables includes the impact surface coefficient of friction (XMU), the critical damping ratio for external springs (CDAMP) which represent crushable structure on the underside of the fuselage, the shock strut friction force (ALPHAP) for special elements of that type, the internal beam damping constant (DAMPC), and the material properties themselves, including the moduli of elasticity and rigidity (EE and GG), and maximum tensile (STENS), compressive (SCOMP), and shear (SHEAR) stresses.

Table 3 Time comparison between models for one run

Model	CPU Time, min
Stick	1:45
Expanded	9:17

Certainly, other input parameters exhibit random behavior as well, such as aerodynamic forces and spring load-deflection data. However, not enough information on these parameters currently exists to model them probabilistically. Conversely, the existing experimental data indicates that the formerly mentioned parameters fall into a well-defined range of values.

The impact surface coefficient of friction ranges between 0.35–0.60 for structure to ground impact. The critical damping ratio for external springs falls between 0.02–0.10. The shock strut friction force ranges from 0.1 to 2.0, and the internal beam damping constant varies from 0.1 to 0.5. Finally, the standard material properties have well established means and standard deviations.[3]

The parameters used in the initial sensitivity study, therefore, are the material properties, the impact surface coefficient of friction, the spring damping ratio, and the beam damping constant. Since the stick model does not contain shock strut elements, this parameter was not studied in the analysis. The materials specified by the model are 2024-T3 aluminum and 6061-T3 aluminum.

C. Results of Sensitivity Analysis

The sensitivity analysis performed here is completely deterministic. The purpose is to identify which parameters have a significant effect on the mass impulse. Responses are calculated for two masses from the model, specifically mass 2 and mass 6 (Fig. 1). The first of these masses represents the worst overall structural case in terms of accelerations and impulses. Mass 6 was chosen since it exhibits the most severe responses in a section where passengers would certainly be located. The distance between the masses is 55 ft in the longitudinal direction. The mass 2 x-direction plots are presented here because as the trends they exhibit are representative of general structural response.

For each of the four variables studied, a measure of the change in value of the impulse was evaluated. The response was examined from a time of 0.085–0.110 s in all cases shown

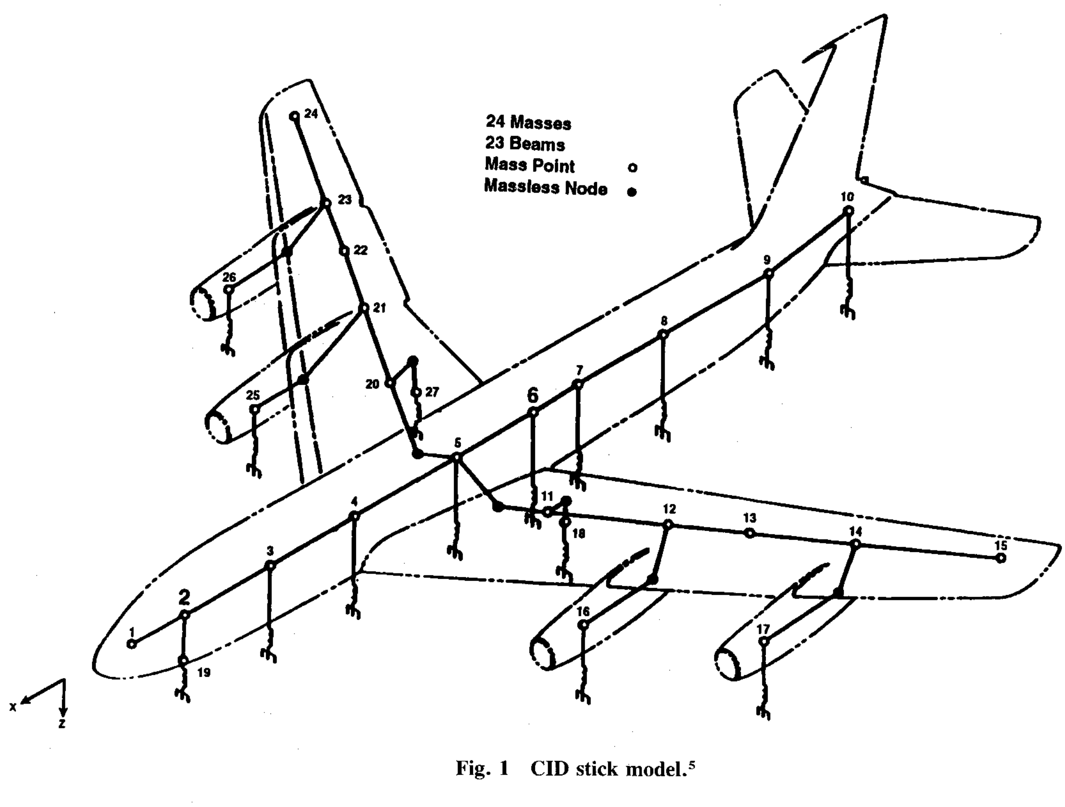

Fig. 1 CID stick model.[5]

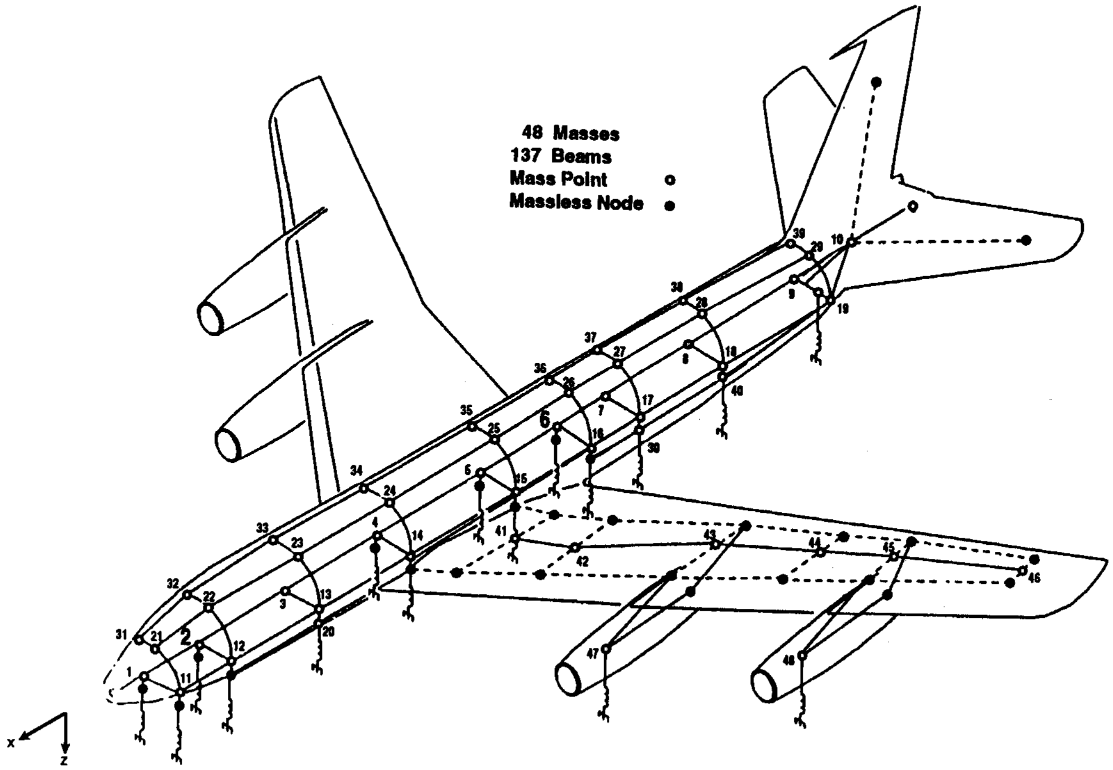

Fig. 2 CID expanded model.[5]

Table 4 Impulse variations

	Mass 2 impulses		Mass 6 impulses	
Parameter	*X* Change	*Z* Change	*X* Change	*Z* Change
Beam damping	43.35%	5.37%	40.91%	1.54%
Spring damping	89.97%	42.13%	212.02%	18.94%
Ground friction	32.28%	1.16%	91.86%	8.31%
Material properties	9.61%	2.82%	25.42%	1.20%

in Table 4. At each 0.005-s interval, the percent change in impulse was calculated. This calculation was based upon the difference in the impulse at the maximum and minimum values of the particular variable being studied. For example, for the beam damping constant, the difference between the impulses was calculated for damping constants of 0.1 and 0.5. A percent change was obtained from this value. The six percentages in the time interval investigated (one for each 0.005-s step) were then averaged to obtain a representation of the general sensitivity of the respective parameters in the given time range. These average variations are listed in Table 4.

The first parameter modified was the internal damping constant. The three cases studied are for damping constants of 0.1, 0.3, and 0.5. The impulse is plotted for mass 2 *x* direction in Fig. 3.

The impulse affected the most in this case was the mass 2 *x* impulse. The change here is about 43%. It can be clearly seen from Table 4 that the impulses are more strongly influenced along the *x* direction than the *z* direction. The largest change in the *z* impulse is 5.37%. This occurs for mass 2.

The second parameter studied was the spring damping ratio. The three cases considered were for ratios of 0.00 (no damping), 0.02, and 0.10. Each of the 12 springs was given the same damping ratio, although each would generally have a different value. The mass 2 *x* impulse is shown in Fig. 4.

Variation in this parameter has the greatest effect on the system response, as expected. The largest change occurs in the mass 6 *x* impulse with a change of over 200%. The *x*-impulse change is also large at almost 90%. Also, the *z* im-

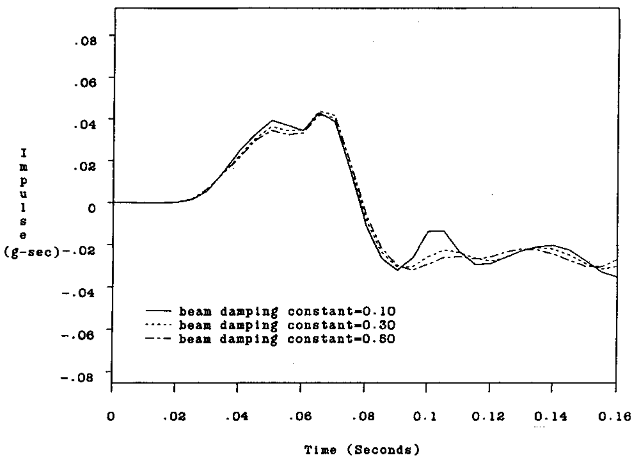

Fig. 3 Mass 2 *x* impulse, internal damping constant.

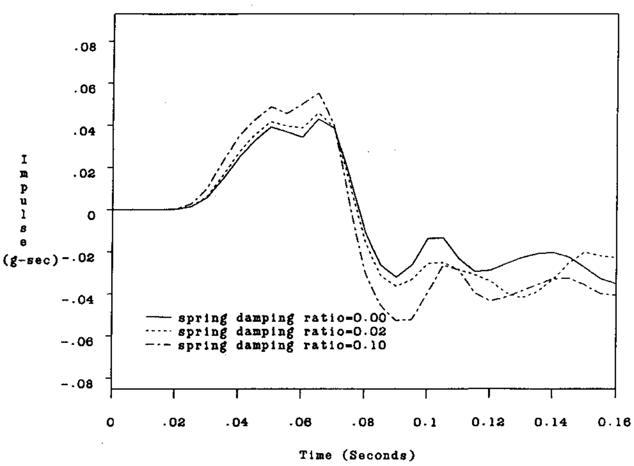

Fig. 4 Mass 2 *x* impulse, spring damping constant.

pulses for both masses exhibit large variations when compared to the responses of the other parameters. The model is therefore most sensitive to changes in the spring damping ratio.

It should be mentioned here that the responses observed are not generally what one would expect from increased damping. That is, the amplitudes of the responses increased with larger damping ratios for the masses studied. It is felt that although this effect is evident here, the amplitudes for other masses decrease for increased damping, particularly for those masses which contact the ground first, near the rear of the model. Also, the overall effect of the increased damping on the model is a decrease in the amplitudes of the responses.

The ground impact coefficient of friction was the third parameter allowed to vary. The values studied were 0.35, 0.5, and 0.6. The impulse is shown in Fig. 5. The effects of the variation in the ground friction can best be seen in the x-direction values for both masses. The change in the impulses here are 32.28 and 91.86%, respectively. Additionally, the mass 6 z impulse has an 8.31% variation, which can also be significant. It has been observed that for a higher coefficient of friction, the impulses are also higher. This can be explained by the higher friction causing a more abrupt deceleration of the masses, and therefore, higher impulses are generated than for a smoother deceleration process with lower friction.

The final parameters varied were the material properties. The material stresses and moduli were first strengthened and then weakened by one standard deviation, respectively. However, since the code permits that only 10 beams could be modeled with nonstandard material properties, the entire structure could not be modified. The beams selected are those which lie along the fuselage, rather than in the wing, as it was felt these beams would have the greatest effect on the masses and floor pulses. The results of this variation are shown in Fig. 6.

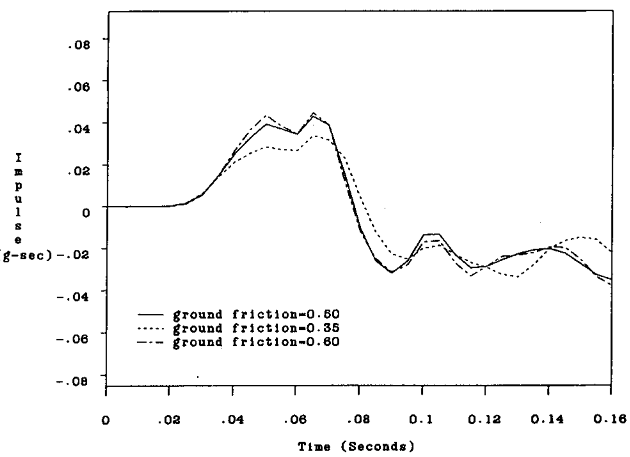

Fig. 5 Mass 2 x impulse, ground friction.

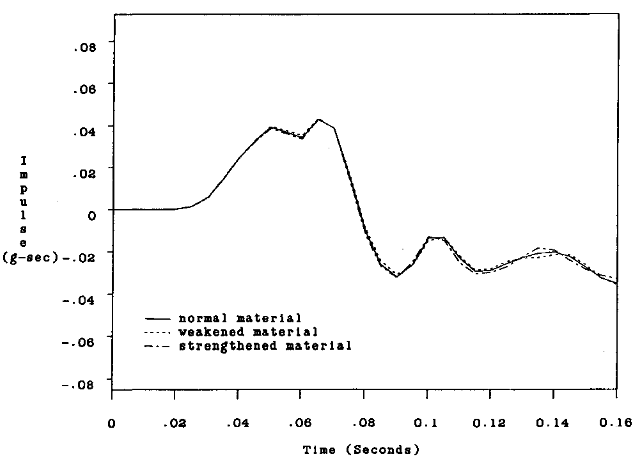

Fig. 6 Mass 2 x impulse, material properties.

The largest change in impulse for this variable is for the mass 6 x direction, at 25.42%. However, all other changes are under 10%. In comparison with results from the other parameters simulated, the model was found to be insensitive to variations in the material properties. This is best illustrated in the z-direction impulses for both masses.

The internal beam damping constant, the spring damping ratio, and the ground impact surface coefficient of friction were all found to affect the responses of the model to some degree. These three parameters, therefore, will be used in the Monte Carlo simulation, which is discussed in Sec. V. Conversely, variations in the material properties were seen to have little effect on the mass responses, and as a consequence the material properties will not be part of this simulation. These properties can, however, be easily added if necessary.

V. Monte Carlo Simulation Results

In this section, results from the Monte Carlo simulation are presented and discussed, including both accelerations and impulses of the two representative masses from the model. Additionally, statistical significance and confidence bounds are demonstrated and calculated respectively.

A. Simulation Results

A Monte Carlo simulation was performed on the CID KRASH stick model as described in Sec. IV.A. The parameters involved in the simulation were the internal beam damping constant, the external spring damping ratio, and the ground coefficient of friction. The simulation consisted of 100 runs of the model. For each run, random values were generated for the three respective variables. Since little information is available on the distributions of the input variables (due to a limited amount of experimental data), each variable used in the simulation was assumed to have a uniform distribution with maximum and minimum values as specified in Sec. IV.B. Only one value of the beam damping constant and friction coefficient were needed for each run, but 12 values of the spring damping ratio were required, one for each of the external springs in the model. It should be noted that although uniform distributions were chosen for this study, the methods employed here may be used for any type of distribution, as appropriate.

The accelerations and impulses were recorded from each run, and a FORTRAN program was written to calculate the means and standard deviations for all quantities at each time step. This is possible because the random behavior modeled is not random in the time domain. These values were then used to make acceleration and impulse plots of the mean response, the mean response ± one standard deviation, and

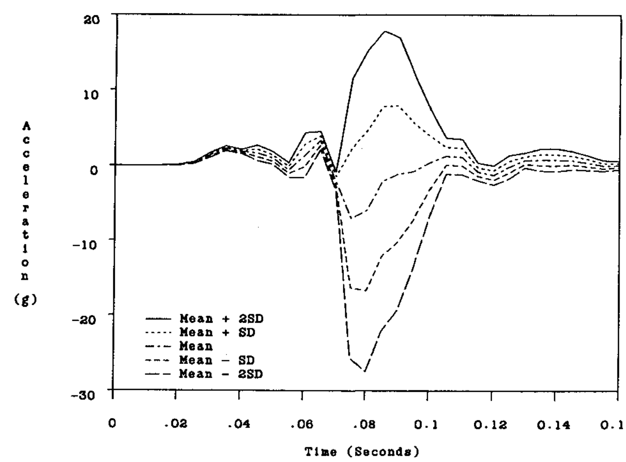

Fig. 7 Mass 2 x acceleration.

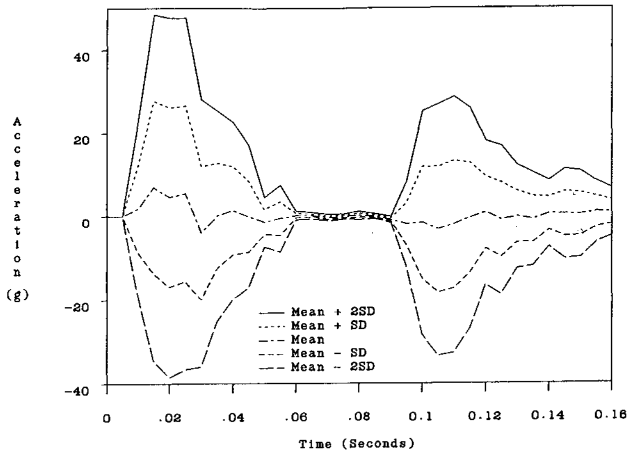

Fig. 8 Mass 6 x acceleration.

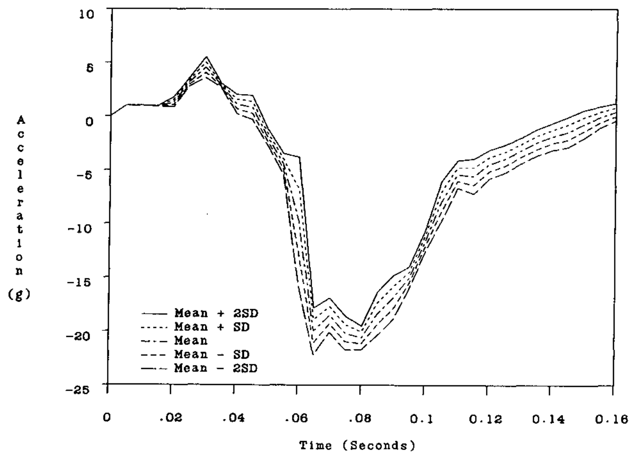

Fig. 9 Mass 2 z acceleration.

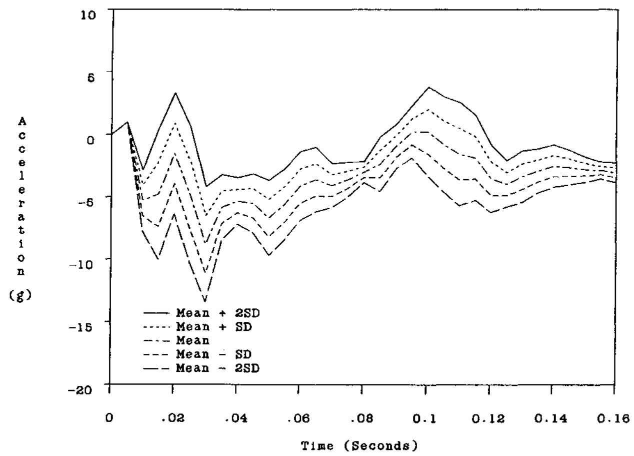

Fig. 10 Mass 6 z acceleration.

the mean response ± two standard deviations. These calculations were performed for masses 2 and 6. The acceleration plots are shown in Figs. 7–10. Attention should be paid to the scales used. Note that all accelerations are in g.

As can be seen from the graphs, the standard deviations in the longitudinal (x) direction are larger than those in the vertical (z) direction, particularly for mass 6. This is primarily due to uncertainty in the mass-ground contact time. For mass 6, there are two areas of large standard deviation. The first of these corresponds to initial ground contact for the mass. The second area is likely a result of ground contact from the nose of the airframe. These uncertainties are reflected in the x-impulse plot as well. Only one area of large standard deviation occurs for mass 2, corresponding to ground contact for that mass. A second possibility for this event is that the longitudinal response is in part owed to coupling with the vertical response. Thus, any change in the vertical pulse is magnified in the longitudinal response. It is believed that the inclusion of longitudinal impact conditions, which could not be done here, would lower the variances in this direction.

An important consideration here is that the existence of these large uncertainties in the acceleration plots would likely be unobserved in a deterministic run of the program, even if two or three different cases were examined. The importance of a probabilistic model is clearly evidenced. Furthermore, an evaluation of the plots indicates that the mean values where the spikes occur are under 5 g in magnitude. Thus, without standard deviations, even a sampling of several runs would not reveal this phenomena.

The pulses shown in Figs. 7–10 are representative KRASH analysis acceleration responses. These are unfiltered accelerations, the reason for which will be explained below. It is not always possible to obtain the peak acceleration directly from these plots, however, as the plot interval may not provide the maximum acceleration value. This is due to the numerical integration scheme, because the time step used in the integration routine may not be small enough to produce this value. It is important to get an accurate measure of this quantity, since this is used to determine occupant response to the impact. An accepted approach to calculate the peak acceleration is to use an equivalent triangular pulse, which is obtained by integrating the acceleration data over the time period of interest.[11] This yields an average acceleration which, when multiplied by two, provides the equivalent peak for a triangular-shaped pulse for the duration of the interval being considered. This representative peak acceleration can be calculated by

$$\text{peak acceleration} = \frac{2 \cdot \text{Impulse}}{\Delta t}, \qquad 0.1 < \Delta t < 0.2 \qquad (2)$$

For a triangular-shaped pulse, the peak normally occurs between 0.1–0.2 s, so this time range is given as a general guideline.

Using the values of the mass impulses (determined by KRASH) and Eq. (2), the mean peak accelerations and their respective standard deviations, are calculated and displayed in Table 5. The presentation of the data in this form provides for a more consistent interpretation of the response. If only peaks are used, the question of whether the peak was actually plotted has to be resolved, as well as how long the peak value is sustained. A further difficulty is that if filtered acceleration data is used, which is often the case for data obtained through structural testing, the filter characteristics (i.e., cutoff frequency and decay rate) can influence the results. The impulse data, therefore, provides a better indication of the overall pulse definition independent of plot interval and filter characteristics.

The calculated peak accelerations are what one would basically expect. The longitudinal peaks are both under 1 g, which can be expected due to the absence of any initial velocity in that direction. The vertical peaks are an order of magnitude larger. The values for mass 2 are higher than those for mass 6 due to the initial pitch attitude of the model. Additionally, the location of mass 2 near the nose of the plane as compared with the location of mass 6 in the midsection of the fuselage would cause one to expect the pulses to be higher there. For

Table 5 Peak acceleration, g

	Longitudinal peak		Vertical peak	
	Mean	Standard deviation	Mean	Standard deviation
Mass 2	0.69	0.08	11.35	0.13
Mass 6	0.38	0.07	6.84	0.06

the vertical peaks, both standard deviations are quite small. This is due to the method of calculating these values by means of the mass impulses. When the standard deviations in the longitudinal direction are examined, however, they are relatively large when compared to the means. Again, it is felt that this is due to the lack of any significant loadings along this direction, causing an increased sensitivity to appear.

B. Statistical Significance

In order for the Monte Carlo simulation results to have meaning, the family of experiments must be large enough to ensure statistical significance. By measuring the statistics of the response (i.e., the means and standard deviations) after a selected number of runs, and then comparing these values to those obtained after more runs have been added to the simulation, a measure of the change in these values can be taken. If these changes are within acceptable tolerances, then one may conclude that the statistical sample size is sufficient. There are quantitative tests for such assurance.

The procedure mentioned above is illustrated in Tables 6–9. The means and standard deviations were calculated after 25, 50, and 100 runs, respectively. The particular values in the tables are for accelerations only, as there was little change in these values for the mass impulses. The time steps shown in Tables 7–9 are for 0.065 and 0.085 s. These time steps were selected to demonstrate that statistical convergence will occur at different rates for different locations and for each time step.

Table 6 Mass 2 sensitivity—0.065 s

	Mean	% Change	Standard deviation	% Change
X Acceleration				
25 Runs	−2.102		0.5532	
50 Runs	−2.098	−0.19	0.6286	13.63
100 Runs	−2.092	−0.29	0.6219	−1.07
Z Acceleration				
25 Runs	−0.538		0.3360	
50 Runs	−0.429	−20.26	0.3615	7.59
100 Runs	−0.411	−4.20	0.3751	3.76

Table 7 Mass 6 sensitivity—0.065 s

	Mean	% Change	Standard deviation	% Change
X Acceleration				
25 Runs	−18.521		0.9403	
50 Runs	−18.589	0.37	0.8412	−10.54
100 Runs	−18.497	−0.49	0.7937	−5.65
Z Acceleration				
25 Runs	−4.192		0.8931	
50 Runs	−4.181	−0.26	0.9447	5.78
100 Runs	−4.082	−2.37	0.8829	−6.54

Table 8 Mass 2 sensitivity—0.085 s

	Mean	% Change	Standard deviation	% Change
X Acceleration				
25 Runs	1.121		9.4005	
50 Runs	−1.175		9.3952	−0.06
100 Runs	−1.138	−3.15	9.0609	−3.56
Z Acceleration				
25 Runs	−16.758		1.1029	
50 Runs	−16.831	0.44	1.0150	−7.97
100 Runs	−16.851	0.12	1.0163	0.13

Table 9 Mass 6 sensitivity—0.085 s

	Mean	% Change	Standard deviation	% Change
X Acceleration				
25 Runs	−0.950		0.3400	
50 Runs	−0.942	0.84	0.3610	6.18
100 Runs	−0.957	1.59	0.3641	0.86
Z Acceleration				
25 Runs	−0.997		0.7886	
50 Runs	−1.039	−4.21	0.8674	9.99
100 Runs	−0.933	10.20	0.8870	2.26

As can be seen from Tables 6 and 7, improvements occur in all values as the number of runs increases, except for the mass 6 z-acceleration standard deviation, which remains at about a 6% change. All other changes are at or below 5%. In contrast, upon examining Tables 8 and 9 the greatest changes occur in the mean values, with the largest difference being approximately 10%. This occurs for the vertical acceleration of mass 6. Although the other three means vary by less than 5%, and the changes in the standard deviations appear to be within reasonable limits, a trend of growth in the changes is observed for the mass 6 means, and the mass 2 x-acceleration standard deviation. This indicates that the 100 run simulation is not sufficient to guarantee statistical significance for every time step. However, since the computational time required to add at least an additional 100 runs to the simulation would be considerable, the 100-run simulation is felt to be acceptable for the purposes of this study.

C. Confidence Bounds

The use of confidence bounds provides a measure of reliability to the results of the simulation. To get a lower bound on our results, Chebyshev's theorem is used. The theorem states that the probability that any random variable X will assume a value within t standard deviations of the mean is at least $1 - (1/t^2)$.[12] Written probabilistically, this means

$$P(\mu - t\sigma < X < \mu + t\sigma) \geq 1 - (1/t^2) \qquad (3)$$

where μ and σ are the mean and standard deviation, respectively.

For $t = 2$ then, there is at least a 0.75 probability of any observation falling within two standard deviations of the mean. This range is shown by the upper and lower lines in Figs. 7–10. It should be noted that while this may be considered a broad statement, the size of the standard deviation at each time step will give a corresponding range of values within which any observation may fall. For example, examining the mass 2 longitudinal acceleration at a time of 0.025 s, we find a minimum 75% probability that any observation will fall between 1.0602–1.6678 g. Conversely, examining the mass 6 longitudinal acceleration at the same time step, we find that the range is −36.047 g to 28.081 g. The first case gives a rather small range of values where an observation is likely to appear, while the second case gives a range of over 60 g. Clearly, the size of the standard deviation is important in determining the usefulness of the confidence bound.

Finally, it should be noted that Chebyshev's theorem is valid for any type of distribution. As a consequence, the results are usually not sharp. The theorem gives a lower bound only, but does not provide any estimate as to how much greater the probability might be above the 75% in this case. Nevertheless, Chebyshev's theorem yields a conservative lower bound upon which a fundamental grasp of how the response will be distributed is obtainable. Only when something is known about the distribution of the observations can the bound be improved upon. Other inequalities may be employed for this purpose.

VI. Conclusions

A Monte Carlo simulation was performed using the KRASH CID stick model. Parameters representing external structure and fuselage properties were varied to determine how they affected the response predictions of the model. The deterministic sensitivity analysis revealed that the internal beam damping constant, the external spring damping ratio, and the ground impact coefficient of friction had the greatest influence on the model.

The simulation was run 100 times. For each run, random numbers were generated for the parameters mentioned above. Each variable was assumed to have a uniform distribution with established ranges (maximum and minimum values). Several values of the spring damping ratio were generated for each run, one for each external spring in the model. The accelerations and mass impulses were recorded at each run for two masses, one located near the nose of the aircraft (mass 2), and the second located near the wing sections (mass 6). The response data was analyzed statistically to obtain the means and standard deviations at each time step.

Statistical significance was investigated to show that convergence will occur at different rates for different time steps. Although the majority of statistics varied by under 5%, it was felt statistical significance was not guaranteed for all the time steps. Nevertheless, the 100-run simulation was determined to be acceptable for the purposes of this study. Plots were presented of the accelerations for the mean response, the mean response ± one standard deviation, and the mean response ± two standard deviations. Peak accelerations were calculated from the impulse data. The peak vertical accelerations were approximately 11 g for mass 2 and approximately 7 g for mass 6. Both longitudinal peak accelerations were under 1 g. These values are consistent with previous test results.

Finally, as an example, confidence bounds were calculated for the responses using Chebyshev's theorem. This gives a conservative lower bound on the pulses. It was shown that any observation has a 75% probability of lying within the upper and lower plots ($\mu \pm 2\sigma$) on each of Figs. 7–10.

Acknowledgments

The authors are pleased to acknowledge the support and interest of the Federal Aviation Administration, and the FAA Technical Center. In particular, the continued support of Larry Neri at the Technical Center is sincerely appreciated.

References

[1]Rubinstein, R. Y., *Simulation and the Monte Carlo Method*, Wiley, New York, 1981.

[2]Shinozuka, M., and Deodatis, G., "Simulation of Stochastic Processes by Spectral Representation," *Applied Mechanics Reviews*, Vol. 44, April 1991, pp. 191–204.

[3]Haugen, E. B., *Probabilistic Mechanical Design*, Wiley, New York, 1980.

[4]Wittlin, G., and LaBarge, B., "KRASH Dynamics Analysis Modeling—Transport Airplane Controlled Impact Demonstration Test," Lockheed-California Co., DOT/FAA/CT-85/9, FAA Technical Center, Atlantic City International Airport, NJ, March 1986.

[5]Wittlin, G., and LaBarge, B., "KRASH Parametric Sensitivity Study—Transport Category Airplanes," Lockheed-California Company, DOT/FAA/CT-87/13, FAA Technical Center, Atlantic City International Airport, NJ, Dec. 1987.

[6]Ang, A. H.-S., and Tang, W. H., *Probability Concepts in Engineering Planning and Design, Volume II: Decision, Risk, and Reliability*, Wiley, New York, 1984.

[7]Hammersley, J. M., and Handscomb, D. C., *Monte Carlo Methods*, Wiley, New York, 1964.

[8]Gamon, M., and Wittlin, G., "Program "KRASH" Theory Manual," Lockheed Aeronautical Systems Co., DOT/FAA/CT-90/25, FAA Technical Center, Atlantic City International Airport, NJ, June 1992.

[9]Press, W. H., Flannery, B. P., Teukpsky, S. A., and Vetterling, W. T., *Numerical Recipes: The Art of Scientific Computing*, Cambridge Univ. Press, New York, 1986.

[10]Hahn, G. J., and Shapiro, S. S., *Statistical Models in Engineering*, Wiley, New York, 1967.

[11]Gamon, M., Wittlin, G., and LaBarge, B., "KRASH 85 User's Guide—Input/Output Format," Lockheed-California Co., DOT/FAA/CT-85/10, FAA Technical Center, Atlantic City International Airport, NJ, March 1986.

[12]Walpole, R. E., and Myers, R. H., *Probability and Statistics for Engineers and Scientists*, Macmillan Publishing Co., New York, 1985.